Visible and Infrared Photometry of Kuiper Belt Objects: Searching for Evidence of Trends.

Neil McBride and Simon F. Green
Planetary and Space Sciences Research Institute
The Open University, Milton Keynes MK7 6AA, United Kingdom
Email: N.M.McBride@open.ac.uk

John K. Davies
Astronomy Technology Centre, Royal Observatory, Blackford Hill, Edinburgh EH9 3HJ, UK

David J. Tholen and Scott S. Sheppard
Institute for Astronomy, Woodlawn Drive, Honolulu, Hawaii, 96822

Robert J. Whiteley
Lunar and Planetary Laboratory, Tucson, Arizona, 85721
AND

Jon K. Hillier
Unit for Space Sciences & Astrophysics, School of Physical Sciences,
University of Kent, Canterbury, CT2 7NR, UK

We present new visible–infrared (V−J) observations of 17 Kuiper Belt objects. 14 of the objects were observed in the visible and infrared wavebands simultaneously to limit the effects of lightcurve variations. Combining these data with our previously published visible–infrared data provides a dataset of 29 objects, 25 of which offer simultaneous V−J colors. We examine the resulting dataset for evidence of relationships between physical properties and orbital characteristics. We find no evidence of a color–size relationship (as previously suspected) at least over the size range sampled. The dataset supports the trend, reported elsewhere, that there is a predominance of red material on the surfaces of objects having perihelia beyond 40 AU. Our data are also supportive, albeit weakly, of a reported correlation between inclination and color in the classical Kuiper Belt — although it is perhaps more correct to say that our data show that there appears to be a lack of low inclination blue objects. Our V−J colors appear broadly correlated with published optical colors, thus suggesting that the surfaces of Kuiper Belt objects are subject to a single reddening agent.

1 INTRODUCTION

As has been extensively described elsewhere (see e.g. Luu and Jewitt 2002), the planetesimals
in the trans-Neptunian region can be regarded as comprising three populations: the Plutinos,
the classical objects and the scattered disk objects. Originally conceived (e.g. Leonard 1930,
Edgeworth 1943, 1949, Kuiper 1951) as a dynamically calm disk of planetesimals left over from
the formation of the Solar System, the discovery of these three populations shows that the
'Kuiper Belt' is in fact much more complicated and holds important clues to the origin of the
Solar System.

Brown (2001) has used discovery statistics to determine that the classical Kuiper Belt may
consist of two populations having different mean inclinations. Levison and Stern (2001) report a
statistically significant relationship between absolute magnitude H_V and inclination i within the
classical Kuiper Belt, with $H_V < 6.5$ objects having significantly higher inclinations than those
with $H_V > 6.5$. They interpret this division as being the superposition of a dynamically cold
primordial population and a collection of (on average) larger objects formed in the inner regions
of the Uranus-Neptune zone and subsequently transported farther outwards during some later
dynamical clearing of the inner disk.

Until recently, attempts to link observable parameters such as color or size with orbital
parameters of the trans-Neptunian objects have been unsuccessful. Jewitt and Luu (1998)
presented 5 objects that appeared to correlate color with absolute magnitude (at the 3 sigma
level), the possible interpretation being that large objects were more blue than small objects.
However as the authors pointed out, the correlation could have been a statistical fluke, and indeed
the larger dataset of optical–infrared colors in Davies *et al.* (2000), and later work by Jewitt and
Luu (2001) did not support a color-size correlation. The bi-modal distribution of colors reported
by Tegler and Romanishin (1998) has not been confirmed by any other group doing similar work
(e.g. Boehnhardt *et al.* 2001, Barucci *et al.* 2001, Delsanti *et al.* 2001, Jewitt and Luu 2001).
However two such trends have now been detected with somewhat higher confidence. Tegler
and Romanishin (2000) report that objects with perihelia beyond 40 AU are systematically
red, and this conclusion is supported at the 3 sigma level by the results of Jewitt and Luu
(2001). Tegler and Romanishin (2000) also note that red classical objects have relatively low
inclinations ($<13°$), and a more explicit correlation between color and inclination in the classical
Kuiper Belt is presented by Trujillo and Brown (2002a). Additionally, Trujillo and Brown note
that this effect had been previously unremarked upon as no such correlation is apparent in the
Plutinos and that the presence of the Plutino data in most other data masks the effect.

These observations hint that clues to the structure of the present trans-Neptunian region
may indeed be found in existing datasets and we wish to test these relationships with new,
unpublished $V-J$ colors of these distant objects. Davies *et al.* (2000) presented J band data
of 14 Kuiper Belt Objects (KBOs) (2 of which were non-detection upper limits) acquired using
the 3.8m United Kingdom Infrared Telescope (UKIRT) while simultaneous V band data were
acquired using the University of Hawaii 2.24m telescope. Using the same techniques we have
expanded this sample to 29 objects (25 of which offer simultaneous $V-J$ data).

2 OBSERVATIONS AND DATA REDUCTION

V band imaging was obtained using the University of Hawaii 2.24m telescope. V band was chosen
as the V-to-J colors give a large spectral range (i.e. greater than R band) and a reasonable signal

to noise for what is predominantly a rather 'red' population of objects (i.e. better than B band). Additionally, spectral reflectance data are usually normalised to V, and thus it allowed easier comparison with other data. The telescope's camera was fitted with a 2048×2048 pixel Tektronix CCD (24 μm pixels) having a 0.219 arcseconds per pixel scale. The field of view was 7.5×7.5 arcminutes. Exposures were between 200 and 900 seconds. The longer exposures were on objects near quadrature where the motion in the plane of the sky was small. Accordingly, trailing was not a factor in any image of the relatively slow moving Kuiper Belt objects. Seeing was moderate to good throughout the runs (typically less than 1–1.5 arcsec). Exposures were taken using a V filter based on the Johnson system, while the telescope was autoguided on a nearby bright star. To derive consistent V magnitudes, and to account for lightcurve variations, multiple frames (between 2 and 20; typically 5) were taken around the J band frames. Thus observations of J and V band images were 'simultaneous' (except where stated), by which we mean that the V band images at least overlapped with the J band integrations. If needed, for objects with rapidly changing lightcurves, V magnitudes were interpolated to the precise mid-frame time of the J band observation.

The images were bias subtracted, and flat-fielded using frames produced using median filtered twilight sky flats. During a sequence of data frames, the telescope pointing was slightly dithered between frames in order minimize the effects of bad pixels repeatedly falling on objects of interest. To increase the signal-to-noise ratio we performed aperture correction photometry by using a small aperture on the KBOs (chosen by determining the frame FWHM — generally the small aperture would be between 0.65 and 0.9 arcseconds in radius) and then both the same small aperture and a larger aperture (typically between 2.4 to 3.3 arcseconds in radius — where the aperture 'growth curve' would be flattening) on a network of nearby brighter field stars in the same image as the KBO, thus defining the 'aperture correction'. We used the large aperture photometry from the field stars to relate them to the Landolt (1992) standard stars for absolute photometric calibration.

Infrared imaging was obtained with the UK Infrared Telescope's facility infrared camera UFTI. The camera is equipped with a 1024×1024 HgCdTe array, with a plate scale of 0.09 arcsec per pixel giving a field of view of 92 arcsec. Images were taken through the standard J infrared filter (1.25 μm). The observations were made and reduced using standard jittering techniques to obtain a median filtered flat-field from the science frames as described in Davies *et al.* (1998). The procedure is virtually identical to that used when using the IRCAM camera (as was used for the data in Davies *et al.* 2000). Aperture correction techniques were also used in the reduction of the J band data to maximize the signal to noise ratio on the faint target objects. Exposure times varied between 9 and 127 minutes depending on the target and the signal to noise required.

3   RESULTS

Table I lists the new J and V band photometry, and aspect data, obtained for 17 objects, of which 14 have simultaneous V and J band photometry. The quoted errors are from statistical uncertainties in the images. Additional uncertainties in photometric calibration might provide a systematic uncertainty of typically ±0.02 mag in the absolute calibration. Objects (15788) 1993 SB and (19299) 1996 SZ$_4$ were reported in the Davies *et al.* (2000) dataset only as non-detection upper limit J magnitudes. In this new dataset, both these objects were detected.

[**Table I, Table II**]

Table II shows the colors and absolute visual magnitudes (H$_V$) values for our 17 newly observed

objects as well as those reported previously in Davies *et al.* (2000). This gives a total sample of V−J data for 29 objects. To calculate H_V from our V band data, a correction to zero phase angle has been made using the H, G system devised for asteroids (Bowell *et al.* 1989). In the past, an assumed value of G=0.15 has usually been adopted for distant minor planets. However, Sheppard and Jewitt (2002) derive G values for several objects over a range of phase angles between $0°$ and $2°$, and find rather steep solutions (i.e. low G values). We adopt a value of G=−0.1, which we feel is a *representative* value for the objects that have reasonably well defined curves (or do not have a large scatter in the data), and, for simplicity, we apply this value to all our objects. In our previous dataset (Davies *et al.* 2000) we used G=0.15, and so values of H_V must be recalculated (presented in Table II). As the phase angles of our observations are generally less than $2°$, the correction to zero phase angle requires a modification of the reduced magnitude of typically less than 0.2 magnitudes. However over a range of $2°$, the *difference* in H_V produced by using G=0.15 as opposed to G=−0.1 amounts to only 0.005 magnitudes. It thus sensible to calculate H_V when combining and comparing observations of Kuiper Belt objects from different epochs or different observers, even though the precise G is not known.

Of the 29 objects in Table II, 4 objects (3 of which appear in Table I) do not have simultaneous V band data. Thus in order to calculate V−J, V magnitudes were calculated using H_V values derived from observations reported elsewhere. For (15788) 1993 SB and (19299) 1996 SZ_4, we have used H_V values derived from the observations reported in Davies *et al.* (2000). For (33340) 1998 VG_{44}, a value of H_V=6.78±0.15 has been used, based on a mean H_V derived from observations reported by Boehnhardt *et al.* (2001) and Doressoundiram *et al.* (2002). For 1997 CQ_{29}, a value of H_V=7.09±0.15 has been used, based on a mean H_V derived from observations reported by Jewitt and Luu (2001) and Boehnhardt *et al.* (2001).

Of the objects in the new dataset (Table I), (26308) 1998 SM_{165}, (20000) Varuna and 2000 GN_{171} display significant lightcurves (Romanishin *et al.* 2001, Jewitt and Sheppard 2002, Sheppard and Jewitt 2002). In fact, the lightcurve behaviour is so significant (Sheppard and Jewitt 2002), that while 'simultaneous' V and J band observations should account for the variations, the magnitude of the objects could change significantly *during* the J band integrations. In this case, the multiple V band frames taken around the J band integrations were used to define the precise lightcurve behaviour, and the V band magnitudes in Table I are interpolations to the mid-frame time of the J band observation. In this way, we make the best attempt we can to derive effectively 'simultaneous' V−J values for these objects.

The J band observations of (29981) 1999 TD_{10} on 2001 Sep 03 and 2001 Sep 04, and of 1999 TC_{36} on 2001 Sep 03 (see Table I), did not have supporting simultaneous V band observations, and so we have not used these observations to derive the V−J values listed in Table II.

4   DISCUSSION

The majority of data presented here benefit from being taken at both visible and infrared wavelengths simultaneously. Non-simultaneous data suffer the ever present risk of being distorted by either color variations with rotation or by lightcurve effects produced by viewing different aspects of a non-spherical object. To date, there is little evidence for color variations with rotation among Kuiper Belt objects (although this may become apparent with further observations), but there is increasing evidence that the effects of shape dominated lightcurves should be taken into account. Until recently it seemed reasonable to assume that the larger objects (e.g. those with H_V<6) would be spherical, but observations of (20000) Varuna have

shown this assumption to be invalid in at least one case (Farnham 2001, Jewitt and Sheppard 2002).

Following the report of Farnham (2001) that (20000) Varuna had a significant lightcurve, Jewitt and Sheppard (2002) have confirmed the existence of a double peaked lightcurve of amplitude 0.42 magnitude and a period of 6.344 hours. They infer that (20000) Varuna is a prolate body, with an axis ratio of 1.5:1 on the plane of the sky, implying (for reasonable material strengths) that it is a rotationally distorted rubble pile. Yet (20000) Varuna is known (Jewitt et $al.$ 2001) to be large; approximately 900 km in equivalent spherical diameter. Therefore the assumption that the largest known KBOs do not have significant lightcurves is clearly invalid in this case. Additionally, as noted in section 3, objects (26308) 1998 SM_{165} and 2000 GN_{171} also display significant lightcurves. Thus it appears that significant lightcurves displayed by KBOs are not uncommon.

Furthermore, the discovery of several binary asteroids in the Kuiper Belt, e.g. 1998 WW_{31} (Veillet 2001), 2001 QT_{297} (Elliot et $al.$ 2001), 2001 QW_{322} (Kavelaars et $al.$ 2001), (26308) 1998 SM_{165} (Brown and Trujillo 2002), 1999 TC_{36} (Trujillo and Brown 2002b), 1997 CQ_{29} and 2000 CF_{105} (Noll et $al.$ 2002) suggest that collisions must have been an important factor in the formation of this region. Thus we see that a continuum of binary objects, distorted rubble piles, and monolithic objects (which may or may not be spherical) must exist in the Kuiper Belt. Of the binary objects, only 1999 TC_{36}, (26308) 1998 SM_{165} and 1997 CQ_{29} are included in our sample. As the separations of the systems are small, typically $\sim$0.2–0.4 arcsec (Brown and Trujillo 2002, Trujillo and Brown 2002b, Marchis and Berthier 2002, Noll et $al.$ 2002) both binary components would be included in our photometric apertures.

Taking the factors mentioned above into account, we conclude that interpretation of non-simultaneous data must be made with care. As an example, we note that in the case of 1997 CQ_{29} our infrared data and that of Boehnhardt et $al.$ (2001) are quite discordant. The H_J values differ by 0.5 magnitudes, which is well outside the likely photometric errors. Noting that the H_V deduced from the data of Boehnhardt et $al.$ (2001) and that of Jewitt and Luu (2001) also differ by 0.2 magnitudes we speculate that this object has a significant lightcurve (although the binary nature of the object may also be complicating matters).

Although the majority of our V and J band data are taken simultaneously, it is instructive to consider the potential consequences of undetected rotational effects. We compared our values of H_V (for consistency, using G=0.15) with those from the literature (Tegler and Romanishin 1998, Jewitt and Luu 2001, Delsanti et $al.$ 2001 and Boehnhardt et $al.$ 2001). Even neglecting objects for which lightcurves have been determined, the general agreement was poor. Only 4 out of 20 objects agreed to within the 0.1 mag which is about that expected given the quoted (typically ±0.05–0.08) errors. The remainder were roughly equally split between values that agreed within 0.11–0.20 (9 out of 20) and to within 0.21–0.45 (7 out of 20). Although some unidentified systematic differences in absolute calibration may account for some of the scatter, the spread appears too large to be attributed $only$ to this effect. Furthermore there was no link between H_V (taken as an analogue of size) and quality of the agreement. Thus the scatter perhaps reflects the presence of as yet undetected lightcurves, supporting the idea that irregularly shaped objects (e.g. non-spherical rubble piles) may be common in the Kuiper Belt.

With the proviso that we should be a bit more cautious of the non-simultaneous observations, we can examine the combined dataset of 29 objects (Table II) in order to investigate some possible trends. Fig. 1 confirms the absence of any relationship between V−J and H_V. Thus, as was indicated by the smaller Davies et $al.$ (2000) sample, the striking linear relationship found by Jewitt and Luu (1998) for 5 objects, must have been a statistical fluke.

[**Figure 1, Figure 2**]

A comparison of color versus perihelion distance is presented in Fig. 2. This figure appears to support the conclusion of Tegler and Romanishin (2001), that objects with perihelion distances greater than about 40 AU are systematically red. However it is worth considering possible selection effects. There are only five objects with $q>39$ AU in our sample, (all five of them having $V-J>1.8$). We have already demonstrated that blue objects are systematically harder for our programme to measure (see Fig. 3 in Davies *et al.* 2000). For example, the detection of objects beyond 40 AU, with $V-J<1.5$ and $H_V>6.5$ would not be possible for typical integration times. And so at first glance, one might conclude that the lack of blue objects beyond 39 AU is simply a consequence of the J band detection threshold discriminating against bluer objects. However, although this effect must operate to some extent, closer inspection of the 5 objects in our sub-sample reveals that the objects (and their H_V values) are: (20000) Varuna ($H_V=3.78$), (19521) Chaos ($H_V=4.92$), 1997 CS_{29} ($H_V=5.56$), 1999 RZ_{253} ($H_V=6.11$) and 1997 CQ_{29} ($H_V=7.09$). So considering the H_V values, it is clear that even if at least 3 of this sub-sample had been particularly blue, we *would* have detected them. If taken in isolation, we might expect that 'picking' our 5 red objects with $q>39$ AU from a population that was evenly split between red and relatively blue, would correspond to a 1 in 32 chance (i.e. approximately a 2 sigma result). Tegler and Romanishin's 9 red objects corresponded to a more convincing 1 in 512 chance. Furthermore, note that our 5 objects are *different* from the objects observed by Tegler and Romanishin. Thus we might tentatively combine the results to indicate that the first 14 objects investigated by both groups were red; corresponding to about a 1 in 16000 chance. In conclusion, our data appears consistent with Tegler and Romanishin's assertion that objects with perihelion distances greater than about 40 AU are systematically red, and considering both sets of results, the trend appears convincing.

[**Figure 3**]

Our data can also be used to test the suggestion of Trujillo and Brown (2002a) of a link between color and inclination amongst the classical Kuiper Belt and Scattered Disk objects (i.e. non-resonance objects). We have 14 such objects in our sample and so the result is less robust than using the larger sample, but the objects are almost all different from those observed by Trujillo and Brown (2002a). Fig. 3 shows that there appears to be a linear trend towards bluer objects, for inclinations $>15°$, perhaps weakly supporting a correlation. However, considering that we only have 5 objects with $i>15°$ (and also remembering the striking $V-J$ versus H_V 'trend' displayed by 5 objects in Jewitt and Luu 1998), we would not suggest that it is significant based on this dataset alone. Perhaps a more useful observation considering the limitations of the dataset, is that our data appear to show a distinct *lack* of blue objects with inclinations $<20°$. As this represents 11 'red' objects, this result appears more robust. If we consider the $<20°$ region only, and as before, conceptually pick the 11 red objects from a distribution which is equally populated by red and blue objects, a complete lack of any blue objects would correspond to approximately a 1 in 2000 chance. As reported by Trujillo and Brown (2002a), no trends are seen amongst the Plutinos. Indeed, while none of the 14 Plutinos in our sample have inclinations $>20°$, they do have a wide range of colors from $V-J=1.2-2.5$.

Trujillo and Brown (2002a) looked closely at the statistics of their data, testing sub-sets of 'equal perihelion distance' and 'equal inclination'. While a color versus inclination trend was observed, they did not see a trend in the color versus perihelion distance within the sub-set, suggesting that the apparent perihelion distance trend is most likely "a spurious correlation induced by sampling bias". Thus the inclination and perihelion distance trends could be manifestations of the same (inclination driven) effect.

If both the trends that our data appear to support (Fig. 2 and Fig. 3) do indeed operate on all objects, i.e. that our objects with $q >39$ AU are red, and there are no blue objects with inclinations below about $i=20°$, then this is clearly saying that 'blue' objects would be limited to a rather small area of inclination-perihelion distance parameter space. We can assess this suggestion using Fig. 4. Fig. 4a shows the inclination versus perihelion distance of all currently known classical and scattered disk objects, taken from the Minor Planets Center database. The data are more or less a scatter plot (with a concentration around the low inclination, $q=40$–44 AU region). We can now plot our data on this type of diagram, but consider whether the objects are 'blue' or 'red'. The division between blue and red is rather arbitrary, but inspection of our data (Figs. 1–3) show that V−J=1.7 is a reasonable value to use. So we define 'blue' objects as having V−J<1.7 and 'red' objects as having V−J>1.7. Fig. 4b shows our data (classical and scattered disk objects) with the blue and red objects clearly highlighted. The behaviour displayed in Figs. 2 and 3 is again seen, with blue objects confined to a region of perihelion distance <39 AU, and inclinations >20°.

[**Figure 4**]

We can also compare this behaviour with other groups' data. We use the data from Tegler and Romanishin (2000) and Trujillo and Brown (2002a) as these are self consistent datasets and are the data that suggested the trends in the first place. Fig. 4c shows the sub-set of classical and scattered objects from the Tegler and Romanishin (2000) sample. The blue-red division of V−J=1.7, corresponds to a V−R color of 0.53 (see below). Although there are fewer points, the data seem to display the same behaviour as our sample. In Fig. 4d we use the data taken by Trujillo and Brown (2002a). In this case the blue-red division of V−J=1.7, corresponds to a B−V color of 0.84 (see below). In this sample, a broad division is suggested in that the blue objects appear in the top left half of the plot. However there clearly are blue objects that extend into the other sectors of the plot. All datasets appear to suggest a paucity of blue objects with low inclinations at large perihelion distances, although this trend appears to be driven mostly by the lack of blue objects at low inclinations in general.

Of course, in Fig. 4d, the data are in terms of B−V color, rather than V−J, and so by splitting the data into blue and red samples, and comparing the results, we are implicitly assuming that the level of reddening seen in the BVR regime is consistent with that seen in the visible–infrared regime. We can investigate this. The relatively large size of our V−J dataset, and the now numerous optical band observations reported in the literature, allows us to investigate whether there is a robust correlation between optical colors (e.g. B−V or V−R) and the optical–infrared color (V−J). A correlation would suggest that the reddening of an object's surface seen at both visible and infrared wavebands would be due to a single reddening agent. To obtain optical colors of the objects in our sample, we utilize the useful compilation by Hainaut and Delsanti (2002) of virtually all published optical photometry. In Fig. 5, we use the mean V−R and B−V values with the associated quoted sigmas shown as error bars, and plot these against our V−J values. There is a broad correlation between both the B−V and V−R, and our V−J colors. We have fitted regression lines to the data in Figs. 5a and 5b, although we exclude two data points in the B−V plot as these appear to have large error bars and anomalous values compared to the rest of the data. The fit in Fig. 5a gives (V−J)=2.772(B−V)−0.619, and the fit in Fig. 5b gives (V−J)=3.374(V−R)−0.079. It is these fits that we used to convert our blue-red division value of V−J=1.7, to the appropriate V−R and B−V values.

[**Figure 5**]

While Fig. 5 shows quite a good overall correlation between the B−V and V−R, with V−J, we can focus on the individual objects over the entire optical–infrared band by converting the data

7

to relative reflectance spectra. This conversion is done in Fig. 6, where all but 3 of the objects have some optical color data taken from Hainaut and Delsanti (2002) to combine with the $V-J$ data. The data are plotted such that the spectra are separated by 1 magnitude for clarity. The objects have been arranged in order of increasing $V-J$, and it is seen that the spectral slopes cover a very wide (and apparently continuous) range indicating neutral to 'ultrared' surfaces (see Jewitt 2002). The overall visual–infrared spectral slopes derived from our $V-J$ data, correlate quite well with the spectral slopes derived from the BVRI optical data. Some notable exceptions are (33340) 1998 VG_{44}, (19299) 1996 SZ_4 and (to some extent) (15788) 1993 SB. It is interesting to note that these are 3 of the 4 objects in our sample for which we could not obtain simultaneous V and J band observations (indicated in Fig. 6 by parentheses around the object name). The 4th 'non-simultaneous' object, 1997 CQ_{29}, does show a self consistent relative reflectance slope, although the large error bar at the J wavelength probably contributes to this impression. The only other striking non-uniform slopes, are displayed by (32929) 1995 QY_9, and to a lesser extent 1996 TS_{66}. It is not apparent why this should be the case, although (32929) 1995 QY_9 does show some lightcurve variation, and while our V and J data for this object (from Davies *et al.* 2000) were obtained simultaneously, it is perhaps possible that some lightcurve effects have affected the optical colors. The 1996 TS_{66} slope could perhaps be interpreted as being consistent with a linear slope considering the size of the error bars at the I and J wavebands.

[Figure 6]

Overall, we would interpret Fig. 6 as indicating a reasonable correlation between the optical band relative reflectance spectra, and the visual–infrared relative reflectance spectra, this in turn supporting the likely presence of a single reddening agent on the surfaces of these Kuiper Belt objects (in agreement with the conclusions of Jewitt and Luu 2001). This interpretation also means that comparing the data in Fig. 4, based on $V-J$, $V-R$ and $B-V$ respectively, appears valid. While the broad correlation between optical and infrared colors might suggest that future investigations need only rely on BVR observations rather than the often more demanding VJ observations (at least, more demanding if it involves two telescopes), the VJ observations have a much superior spectral range and so are likely to be more robust in showing color correlations. Furthermore, there is always the chance that the individual cases where the optical-infrared spectral slopes do not agree, are actually displaying some undetermined 'interesting' physical behaviour.

Finally, having looked at the possible trends in our data, and found that there appears to be a lack of blue objects at low inclinations, we can consider why this might be the case. If the objects in the Kuiper Belt formed with similar composition, and the predominantly red colors observed are a result of long term irradiation, then the blue objects must have either (i) been prevented from becoming red, or (ii) have suffered some 'blueing' mechanism relatively recently (i.e. on a time scale short compared to the reddening process). Both these scenarios *might* be satisfied by impacts, where a significant amount of sub-surface material is excavated, causing a re-surfacing with more icy ('blue') material. Indeed Stern (1995) suggested that, in this way, one might expect a correlation between color and average impact velocity, and as highlighted by Trujillo and Brown (2002a), the mechanism could be a strong function of orbital inclination. The behaviour of our data (see Fig. 3) broadly supports this in that bluer objects only appear at the higher inclinations, where mean impact velocities within the population are (currently) higher. However as impact probabilities are related to the cross sectional area of the objects, one might expect a correlation between color and size (i.e. H_V). Our data (Fig. 1) do not show this, perhaps arguing against impact resurfacing as the driver for the KBO color behaviour. However, when considering *only* the classical/scattered populations, our data extend over a H_V range of just 2.5 magnitudes, which is only a factor of $\sim$3 in diameter (indeed we are unable

to adequately test the relationship between inclination and H_V proposed by Levison and Stern (2001) for this reason). And so while our data show no apparent correlation between color and H_V, it remains to be seen if any trends become apparent in the classical population when objects ranging over a much wider size range are ultimately observed.

5   CONCLUSIONS

We have presented new (mostly simultaneous) V−J colors that support the color and perihelion distance relationship proposed by Tegler and Romanishin (2001). Our data are also broadly consistent with the color and inclination relationship shown by Trujillo and Brown (2002a), although a more robust conclusion is that there is a paucity of low inclination blue objects.

The published values of absolute magnitude H_V produced by numerous groups appear more inconsistent than would be expected (even considering systematic differences between datasets), which perhaps suggests that large (>0.2 magnitude) lightcurve or other non-periodic variations are quite common even amongst what are thought to be relatively large objects. This inconsistency may indicate that a number of even the larger objects are either non-spherical or suffer periodic outbursts (as proposed for (19308) 1996 TO$_{66}$ by Hainaut *et al.* 2000).

Our V−J colors appear broadly correlated with published optical colors, thus supporting the suggestion that the surface of Kuiper Belt objects are subject to a single reddening agent.

ACKNOWLEDGEMENTS

REFERENCES

Barucci, M.A., M. Fulchignoni, M. Birlan, A. Doressoundiram, J. Romon, and H Boehnhardt 2001. Analysis of Trans-Neptunian and Centaur colours: continuous trend or grouping? *Astron. Astrophys.* **371** 1150–1154.

Boehnhardt, H., G.P. Tozzi, K. Birkle, O. Hainaut, T. Sekiguchi, M. Vair, J. Watanabe, and G.Rupprecht 2001. Visible and near-IR observations of trans-Neptunian Objects. Results from ESO and Calar Alto Telescopes. *Astron. Astrophys.* **378** 653–667.

Bowell, E., B. Hapke, D. Domingue, K. Lumme, J. Peltoniemi, and A.W. Harris 1989. Application of photometric models to asteroids. In *Asteroids II* (R.P. Binzel, T. Gehrels and M.S. Matthews Eds.), pp. 524–556 (equations A4 on p. 550). University of Arizon Press, Tucson.

Brown, M.E. 2001. The inclination distribution of the Kuiper Belt. *Astrophys. J.* **121** 2804–2814.

Brown, M.E., and C. Trujillo 2002. IAC Circular 7807 (January 14).

Davies, J.K., N. McBride, S.E. Ellison, S.F. Green, and D. Ballantyne 1998. Visible and infrared observations of six Centaurs. *Icarus* **134**, 213–227.

Davies, J.K., S. Green, N. McBride, E. Muzzerall, D.J. Tholen, R.J. Whiteley, and J.K. Hillier 2000. Visible and Infrared Photometry of Fourteen Kuiper Belt Objects. *Icarus* **146**, 253–262.

Delsanti, A.C., H. Boehnhardt, L. Barrera, K.J. Meech, T. Sekiguchi, and O.R. Hainaut 2001. BVRI Photometry of 27 Kuiper Belt Objects with ESO Very large Telescope. *Astron. Astrophys.* **380** 347–358.

Doressoundiram, A., M.A. Barucci, J. Romon, and C. Veillet 2002. Multicolor photometry of trans-Neptunian objects. In press.

Edgeworth, K.E. 1943. The evolution of our planetary system. *J. Brit. Astron. Assoc.*, **53**, 181–188.

Edgeworth, K.E. 1949. The origin and evolution of the solar system. *Mon. Not. R. astr. Soc.* **109**, 601–609.

Elliot, J., S. Kern, D. Osip, and S. Burles 2001. IAUC Circular 7733, (October 15).

Farnham, T. 2001. IAU Circular 7583 (February 16).

Hainaut, O.R., C.E. Delahodde, H. Boehnhardt, E. Dotto, M.A. Barruci, K.J. Meech, J.M. Bauer, R.M. West, and A. Doressoundiram 2000. Physical properties of TNO 1999 TO$_{66}$. *Astron. Astrophys.* **356**, 1076–1088.

Hainaut, O.R., and A.C. Delsanti 2002. Colors of minor bodies in the outer Solar System — A statistical analysis. *Astron. Astrophys.* In press.

Jewitt, D.C. 2002. From Kuiper Belt object to cometary nucleus: the missing ultrared matter. *Astron. J.* **123** 1039–1049.

Jewitt, D., and J. Luu 1998. Optical–Infrared Spectral Diversity in the Kuiper Belt. *Astron. J.* **115** 1667–1670.

Jewitt, D., and J. Luu 2001. Colors and Spectra of Kuiper Belt Objects. *Astron. J.* **122** 2099–2114.

Jewitt, D., and S.S. Sheppard 2002. *Astrophys. J.* in press.

Jewitt, D., H. Aussel, and A. Evans 2001. The size and albedo of the Kuiper Belt object (20000) Varuna. *Nature* **411**, 446–447.

Kavelaars J, J. Petit, B. Gladman, and M. Holman 2001. IAU Circular 7749 (November 9).

Kuiper, G.P. 1951. In *Astrophysics* (J.A. Hynek Ed). McGraw Hill, New York 357.

Landolt, A.U. 1992. UBVRI photometric standard stars in the magnitude range 11.5<V<16.0 around the celestial equator. *Astron. J.* **104**, 340–371.

Leonard, F.C. 1930. The new planet Pluto. *Leaflet Astron. Soc. Pac.* No. 30, 121-124.

Levison H.F., and S.A. Stern 2001. On the Size Dependence of the Inclination Distribution of the Main Kuiper Belt. *Astron. J.* **121**, 1730–1735.

Luu, J.X. and D.C. Jewitt 2002. Trans-Neptunian Objects: relics from the accretion disk of the Sun. *Ann. Rev. Astronomy & Astrophysics*, in press.

Marchis, F., and J. Berthier 2002. IAC Circular 7807 (January 24).

Noll, K.S., D.C. Stephens, W.M. Grundy, R.L. Millis, J. Spencer, M. Buie, S.C. Tegler, W. Romanishin and D.P. Cruikshank 2002. Detection of two binary trans-neptunian objects, 1997 CQ_{29} and 2000 CF_{105}, with the Hubble Space Telescope. *Astron. J.* submitted.

Romanishin, W., S.C. Tegler, T.W. Rettig, G. Consolmagno, and B. Botthof 2001. 1998 SM165: A large Kuiper Belt object with an irregular shape. *Procs. of the National Academy of Sciences of the United States of America* **98**, 11863–11866.

Sheppard, S.S., and D.C. Jewitt, 2002. Time-resolved photometry of Kuiper Belt Objects: rotations, shapes, and phase functions. *Astron. J.* **124**, 1757–1775.

Stern, S.A. 1995. Collisional time scales in the Kuiper Disk and their implications. *Astrophys. J.* **110**, 856–868.

Tegler, S.C., and W. Romanishin 1998. Two distinct populations of Kuiper Belt Objects. *Nature* **392**, 49–51.

Tegler, S.C., and W. Romanishin 2000. Extrememly red Kuiper-belt objects in near-circular orbits beyond 40 AU. *Nature* **407**, 979–980.

Trujillo, C., and M. Brown 2002a. A correlation between inclination and color in the classical Kuiper Belt. In press.

Trujillo, C., and M. Brown 2002b. IAC Circular 7787 (January 10).

Veillet, C. 2001. IAU Circular 7610 (April 16).

TABLE I
New Infrared and Visible Band Observations

Object		UT	R (AU)	Δ (AU)	$\alpha°$	J Mag	V mag
	1999 RZ$_{253}$	2000 Oct 2.2493	40.906	40.165	0.947	20.32±0.06	22.33±0.03
(35671)	1998 SN$_{165}$	2000 Oct 2.3219	38.156	37.188	0.376	20.35±0.04	21.62±0.03
(29981)	1999 TD$_{10}$	2000 Oct 3.4090	12.393	11.394	0.226	18.01±0.04	19.80±0.04
		2000 Oct 3.4233				17.98±0.04	
		2001 Sep 3.6102	12.675	11.883	2.921	18.38±0.04	
		2001 Sep 4.6303	12.676	11.873	2.857	18.29±0.04	
	1999 TC$_{36}$	2000 Oct 3.4340	31.537	30.570	0.471	18.14±0.06	20.46±0.03
		2001 Sep 3.4333	31.423	30.484	0.687	18.22±0.04	
(26308)	1998 SM$_{165}$	2000 Oct 3.4872	34.693	33.696	0.130	18.97±0.04	21.35±0.03
(24835)	1995 SM$_{55}$	2000 Oct 3.5608	39.408	38.465	0.495	19.66±0.04	20.67±0.03
(33340)	1998 VG$_{44}$	2000 Oct 3.6003	30.334	29.687	1.462	19.97±0.08	[1]21.77±0.15
(19299)	1996 SZ$_{4}$	2000 Oct 4.4295	29.999	29.010	0.302	21.72±0.10	[2]23.15±0.09
		2000 Oct 4.4833				21.63±0.10	
(15788)	1993 SB	2000 Oct 7.5208	30.499	29.500	0.035	21.62±0.10	[2]23.05±0.05
(38628)	2000 EB$_{173}$	2001 Apr 22.4658	29.745	28.772	0.494	17.91±0.04	19.88±0.03
	1998 HK$_{151}$	2001 Apr 22.5238	30.401	29.489	0.816	20.79±0.07	22.36±0.06
(44594)	1999 OX$_{3}$	2001 Apr 22.6063	27.036	27.129	2.119	19.97±0.06	22.08±0.06
(20000)	Varuna	2001 Apr 22.2842	43.063	43.449	1.231	18.31±0.04	20.32±0.03
	2000 GN$_{171}$	2001 Apr 22.3558	28.800	27.827	0.507	19.50±0.05	21.24±0.03
		2001 Apr 23.4308	28.799	27.831	0.544	19.59±0.05	21.38±0.03
(26181)	1996 GQ$_{21}$	2001 Apr 22.4158	39.277	38.274	0.109	18.57±0.05	21.04±0.03
		2001 Apr 23.4688	39.278	38.275	0.113	18.60±0.04	21.01±0.03
(26375)	1999 DE$_{9}$	2001 Apr 23.3971	33.997	33.457	1.437	18.71±0.06	20.60±0.03
	2000 KK$_{4}$	2001 Apr 23.5679	44.239	43.407	0.744	21.22±0.08	23.01±0.07

Note: All V magnitudes obtained simultaneously with J magnitudes, except: [1]V magnitude calculated from a mean of observations reported by Boehnhardt *et al.* (2002) and Doressoundiram *et al.* (2002), corrected to our values of R, Δ and α. [2]V magnitude calculated from H_V from Davies *et al.* (2000). UT times refer to the J band mid-frame times.

TABLE II
Combined Visible–Infrared (V−J) Dataset

Object		Type	q (AU)	i (deg)	H_V	V−J	Notes
(15788)	1993 SB	P	26.74	1.94	8.27±0.05	1.43±0.11	V derived from H_V
(15789)	1993 SC	P	32.30	5.16	7.37±0.05	2.57±0.08	Simultaneous V−J
(15820)	1994 TB	P	26.95	12.15	8.03±0.05	2.54±0.11	Simultaneous V−J
(32929)	1995 QY$_9$	P	29.20	4.84	7.97±0.04	2.01±0.13	Simultaneous V−J
(24835)	1995 SM$_{55}$	C	37.45	27.01	4.69±0.04	1.01±0.05	Simultaneous V−J
(26181)	1996 GQ$_{21}$	S	38.21	13.37	5.12±0.04	2.44±0.06	Simultaneous V−J
(19299)	1996 SZ$_4$	P	29.36	4.74	8.40±0.09	1.48±0.13	V derived from H_V
(15874)	1996 TL$_{66}$	S	35.03	23.94	5.46±0.02	1.37±0.06	Simultaneous V−J
(19308)	1996 TO$_{66}$	C	38.37	27.43	4.61±0.04	1.00±0.10	Simultaneous V−J
(15875)	1996 TP$_{66}$	P	26.37	5.67	7.41±0.03	2.11±0.06	Simultaneous V−J
	1996 TQ$_{66}$	P	34.61	14.66	7.49±0.06	2.41±0.08	Simultaneous V−J
	1996 TS$_{66}$	C	38.32	7.33	6.61±0.06	1.83±0.11	Simultaneous V−J
	1997 CQ$_{29}$	C	39.76	2.90	[2]7.09±0.15	[2]2.20±0.28	V derived from H_V
	1997 CS$_{29}$	C	43.50	2.23	5.56±0.05	2.06±0.03	Simultaneous V−J
(24952)	1997 QJ$_4$	P	30.43	16.58	7.87±0.11	1.23±0.31	Simultaneous V−J
	1998 HK$_{151}$	P	30.37	5.95	7.47±0.06	1.57±0.09	Simultaneous V−J
(26308)	1998 SM$_{165}$	1:2	30.08	13.49	5.99±0.04	2.38±0.05	Simultaneous V−J
(35671)	1998 SN$_{165}$	P	36.21	4.60	5.80±0.04	1.27±0.05	Simultaneous V−J
(33340)	1998 VG$_{44}$	P	29.38	3.04	[1]6.78±0.15	1.80±0.17	V derived from H_V
(26375)	1999 DE$_9$	S	32.24	7.61	5.11±0.04	1.89±0.07	Simultaneous V−J
(44594)	1999 OX$_3$	S	17.51	2.63	7.46±0.07	2.11±0.08	Simultaneous V−J
	1999 RZ$_{253}$	C	39.89	0.56	6.11±0.04	2.01±0.07	Simultaneous V−J
	1999 TC$_{36}$	P	30.59	8.42	5.46±0.04	2.32±0.07	Simultaneous V−J
(29981)	1999 TD$_{10}$	S	12.30	5.96	9.01±0.05	1.81±0.06	Simultaneous V−J
(38628)	2000 EB$_{173}$	P	28.55	15.47	5.14±0.04	1.97±0.05	Simultaneous V−J
	2000 GN$_{171}$	P	28.30	10.84	6.71±0.04	1.77±0.06	Simultaneous V−J
	2000 KK$_4$	C	37.49	19.13	6.48±0.07	1.79±0.11	Simultaneous V−J
(19521)	Chaos	C	41.05	12.01	4.92±0.04	1.83±0.03	Simultaneous V−J
(20000)	Varuna	C	40.92	17.12	3.78±0.04	2.01±0.05	Simultaneous V−J

Note: H_V values to be used with G=−0.1 (using the H, G relations of Bowell *et al.* 1989). Data are from this work and following Davies *et al.* (2000), except: [1]H_V calculated from a mean of observations reported by Boehnhardt *et al.* (2002) and Doressoundiram *et al.* (2002). [2]H_V calculated from a mean of observations reported by Boehnhardt *et al.* (2002) and Jewitt and Luu (2001). Note (20000) Varuna and (19521) Chaos had the original designations 2000 WR$_{106}$ 1998 WH$_{24}$ respectively.
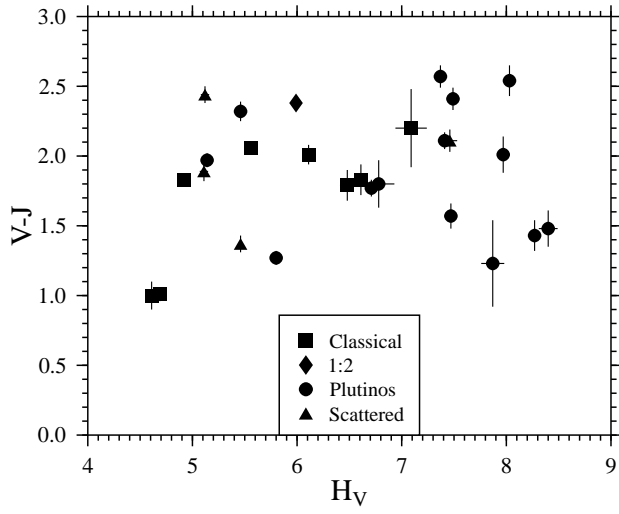
FIG. 1. The V−J color versus the absolute visual magnitude H_V for 29 Kuiper Belt objects.
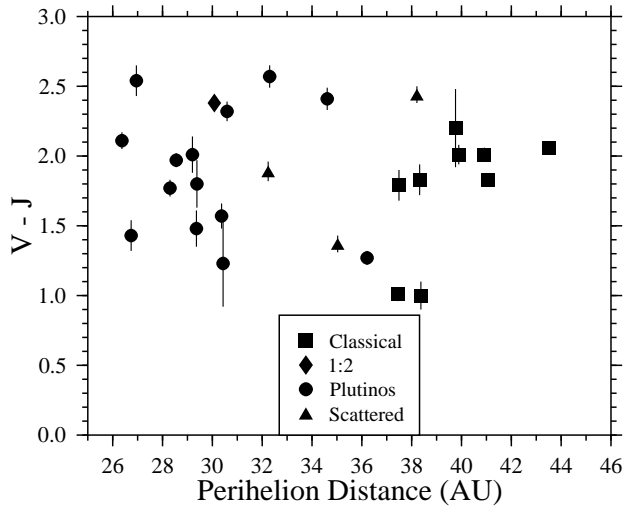
FIG. 2. The V−J color versus the perihelion distance for our sample of 29 Kuiper Belt objects. The small number of objects beyond 39 AU all appear to be red.
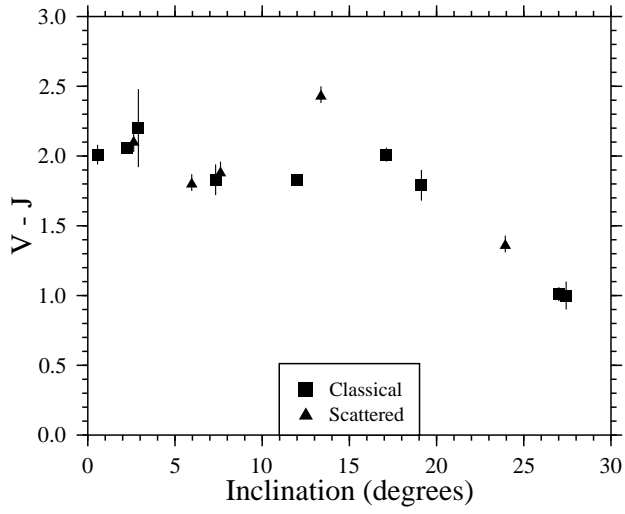
McBride *et al.* Visible and Infrared Photometry of Kuiper Belt Objects: Searching for Evidence of Trends.

FIG. 3. The V−J color versus the inclination for our sample of classical and scattered disk Kuiper Belt objects (excluding the resonant objects).
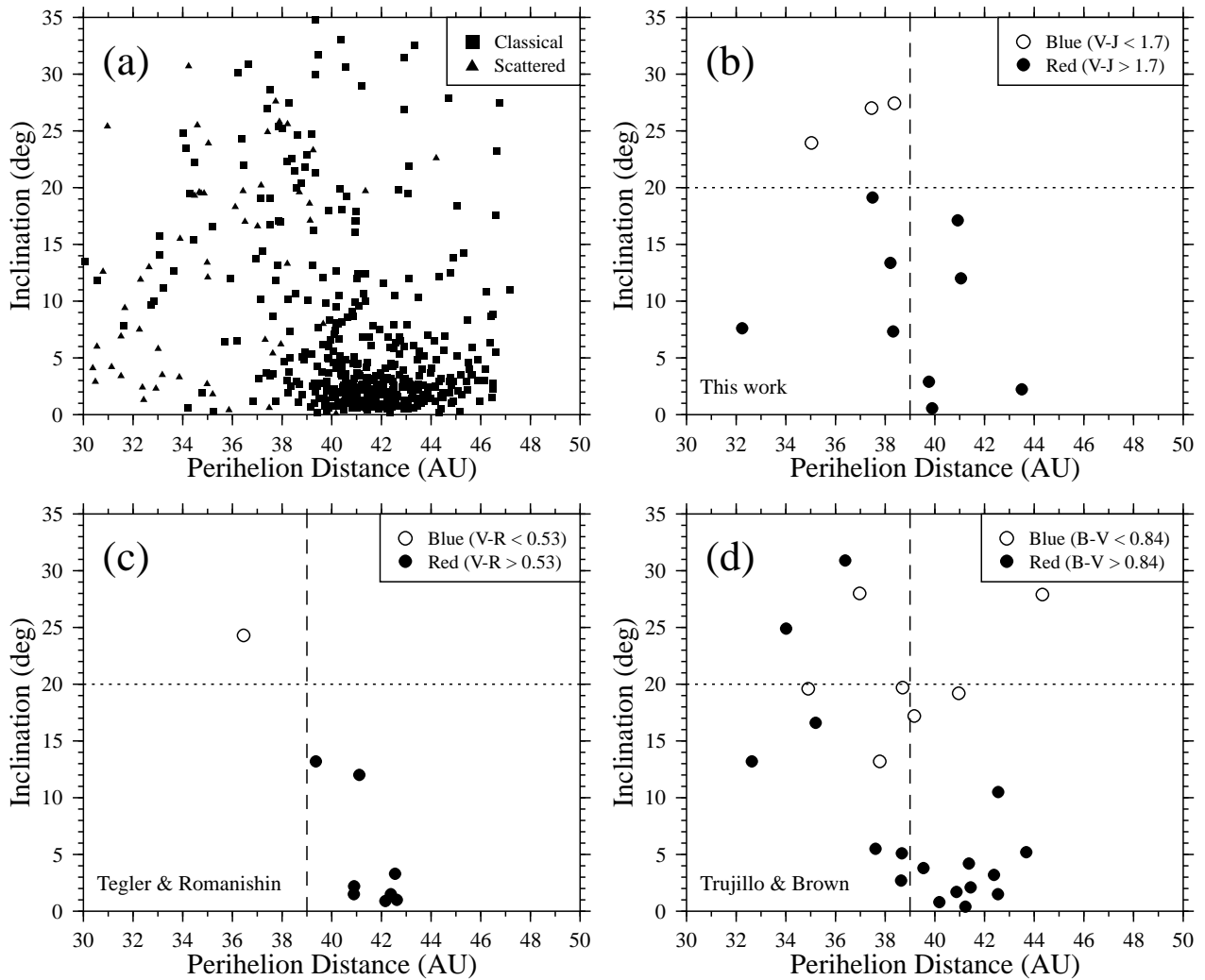
FIG. 4. Inclination versus perihelion distance for non-resonant objects (i.e. classical and scattered disk objects). Error bars have been emitted for clarity. (a) All objects currently listed on the MPC database. (b) Our data. The arbitrary division between 'blue' and 'red' objects has been set at V−J=1.7. (c) Data taken by Tegler and Romanishin (2000). The V−J=1.7 blue-red division corresponds to a V−R color of 0.53. (d) Data taken by Trujillo and Brown (2002a). The V−J=1.7 blue-red division corresponds to a B−V color of 0.84.
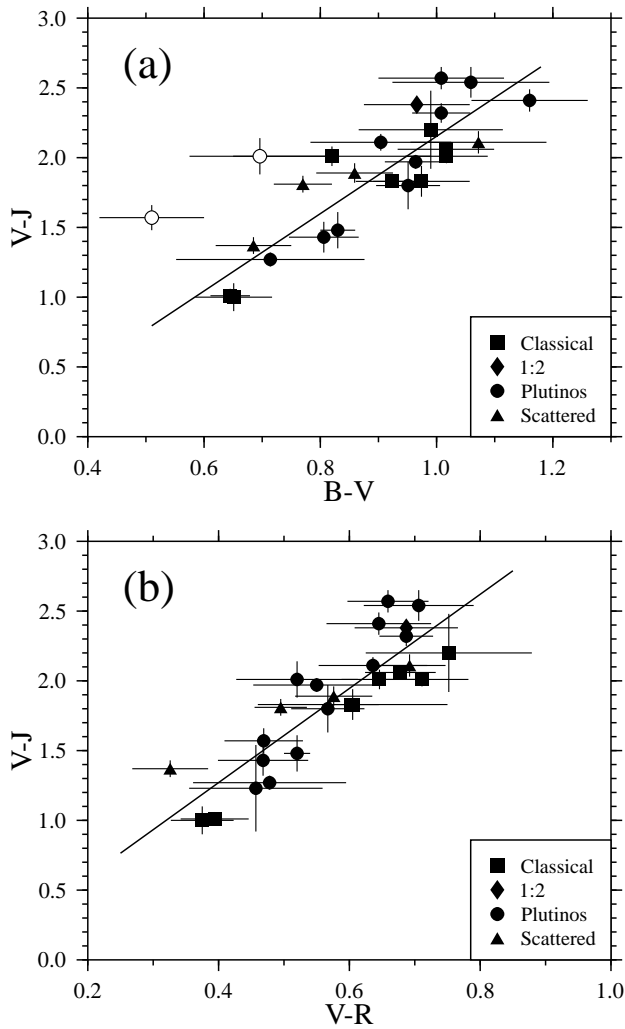
FIG. 5. Our data (V−J) compared with the mean colors listed in Hainaut and Delsanti (2002). (a) V−J versus B−V. The two open circles have been excluded from the fit. The fit gives (V−J)=2.774(B−V)−0.622 (regression coefficient 0.87). (b) V−J versus V−R. The fit gives (V−J)=3.383(V−R)−0.085 (regression coefficient 0.87).
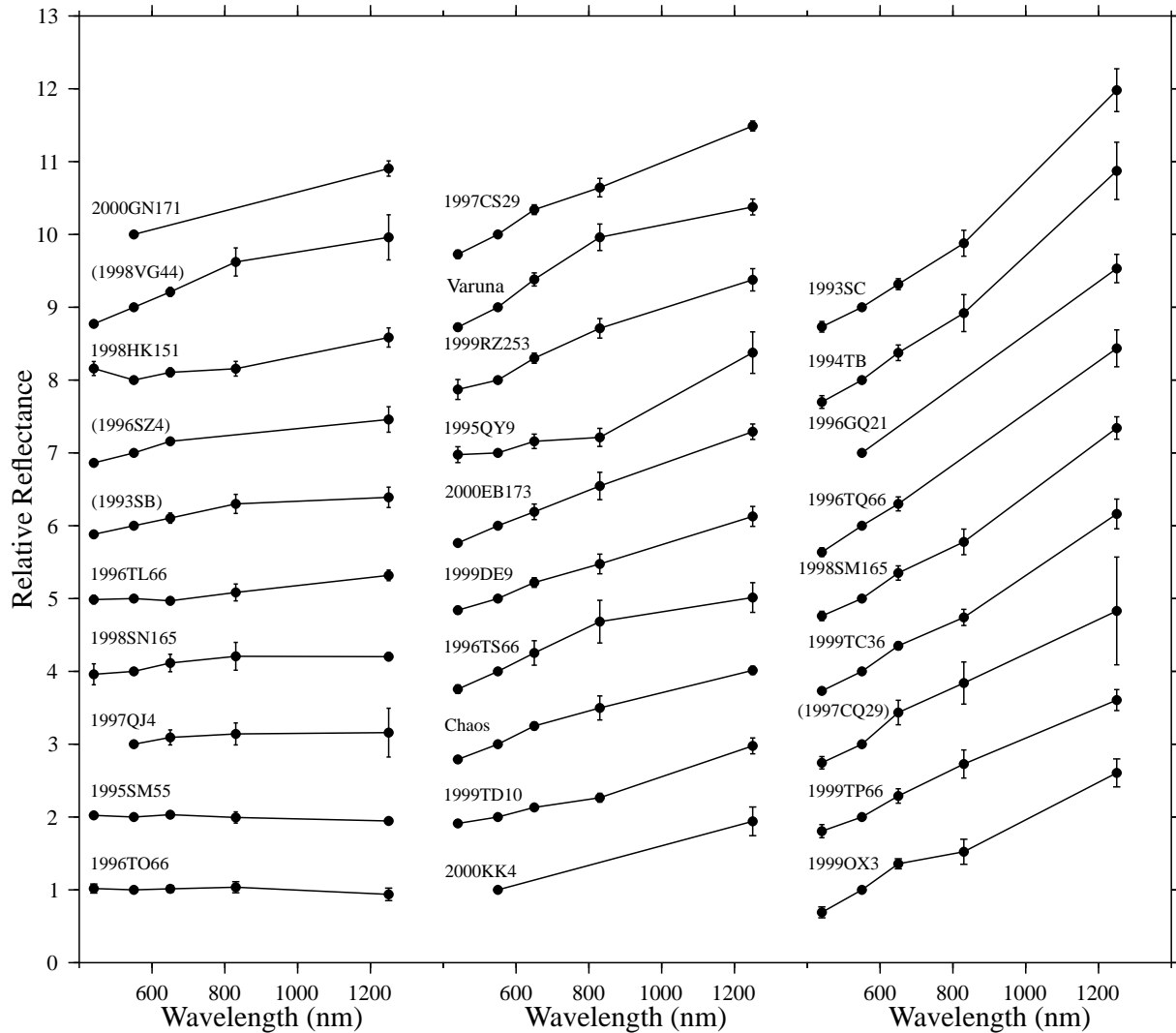
FIG. 6. The relative reflectance spectra of the 29 Kuiper Belt objects, produced by the combination of our V−J colors (simultaneous V−J except for objects in parentheses) with the mean optical colors compiled by Hainaut and Delsanti (2002).